The Triggering mechanism of quiet-region coronal jet eruptions: Flux Cancelation

Navdeep K. Panesar[1], Alphonse C. Sterling[1], and Ronald L. Moore[1,2]

[1]Heliophysics and Planetary Science Office, ZP13, Marshall Space Flight Center, Huntsville, AL

[2]Center for Space Plasma and Aeronomic Research (CSPAR), UAH, Huntsville, AL

Abstract

Coronal jets are frequent transient features on the Sun, observed in EUV and X-ray emissions[1,2]. They occur in active regions, quiet Sun and coronal holes, and appear as a bright spire with base brightenings. Recent studies show that many coronal jets are driven by the eruption of a *minifilament*[3]. Here we investigate the magnetic cause of jet-driving minifilament eruptions. We study ten randomly-found on-disk quiet-region coronal jets using SDO/AIA intensity images and SDO/HMI magnetograms. For all ten events, we track the evolution of photospheric magnetic flux in the jet-base region in EUV images and find that (a) a cool (transition-region temperature) minifilament is present prior to each jet eruption; (b) the pre-eruption minifilament resides above the polarity-inversion line between majority-polarity and minority-polarity magnetic flux patches; (c) the opposite-polarity flux patches converge and cancel with each other; (d) the cancelation between the majority-polarity and minority-polarity flux patches eventually destabilizes the field holding the minifilament to erupt outwards; (e) the envelope of the erupting field barges into ambient oppositely-directed far-reaching field and undergoes external reconnection (interchange reconnection); (f) the external reconnection opens the envelope field and the minifilament field inside, allowing reconnected-heated hot material and cool minifilament material to escape along the far-reaching field, producing the jet spire. In summary, we found that each of our ten jets resulted from a minifilament eruption following flux cancelation at the magnetic neutral line under the pre-eruption minifilament. These observations show that flux cancelation is usually the trigger of quiet-region coronal jet eruptions[4].

Evolution of a Minifilament and Jet

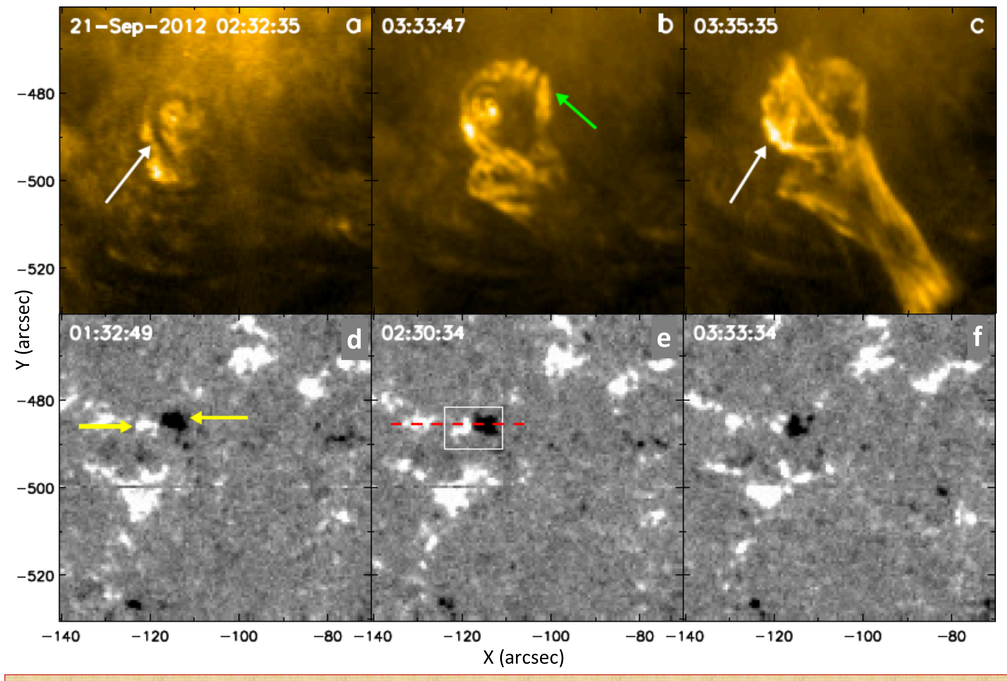

Fig.1. Quiet-region jet (J7) : (a-c) SDO/AIA 171 Å intensity images. (d-f) SDO/HMI magnetograms. The white arrows in (a) and (c) show the minifilament and jet bright point, respectively. The green arrow in (b) points to brightenings from external reconnection. The yellow arrows in (d) show the converging positive and negative flux clumps. In (e) the white boxed region shows the area measured for the magnetic flux-time plot in Fig 2(a) and the red dashed line shows the east-west cut for the time-distance map of Fig. 3(b)

Magnetic field

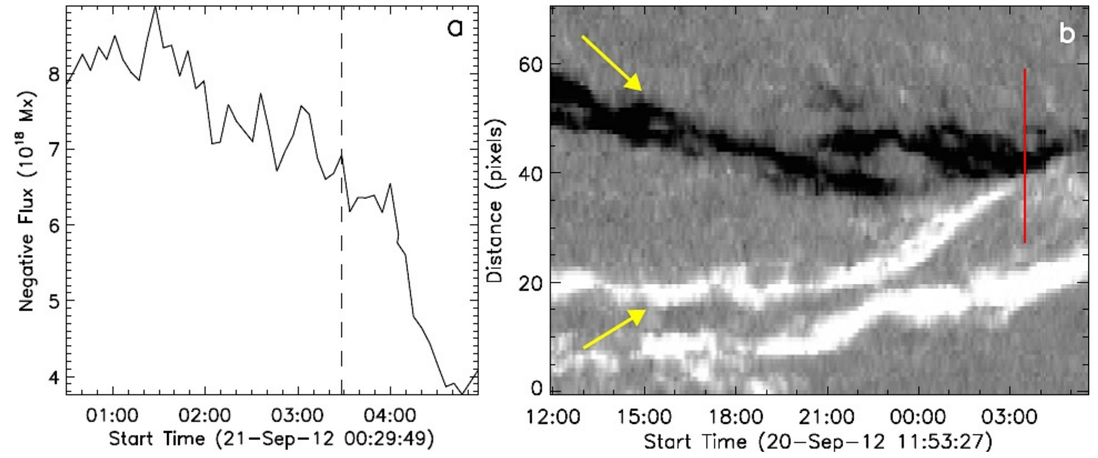

Fig 2. Magnetic flux evolution of jet J7: Panel (a) shows the negative flux as a function of time from inside the box of Fig. 1(e). The dashed line shows the jet eruption time. Panel (b) shows the time-distance map of magnetic flux along the red dashed line of Fig. 1(e). The yellow arrows point to the flux patches that converged and canceled over ~ 18 hours before jet eruption. The red line shows the jet eruption time (03:33 UT).

Interpretation

- The minifilament (blue) initially resides between patches of majority (positive) and minority (negative) flux.
- These two flux patches converge and cancel with each other.
- Continuous flux cancelation at the neutral line apparently destabilizes the filament field to erupt outwards and undergo external reconnection with the surrounding coronal field. The external reconnection opens the overlying field, allowing hot reconnection-heated material and cool minifilament material to escape along the far-reaching field, which appears as part of the jet spire.

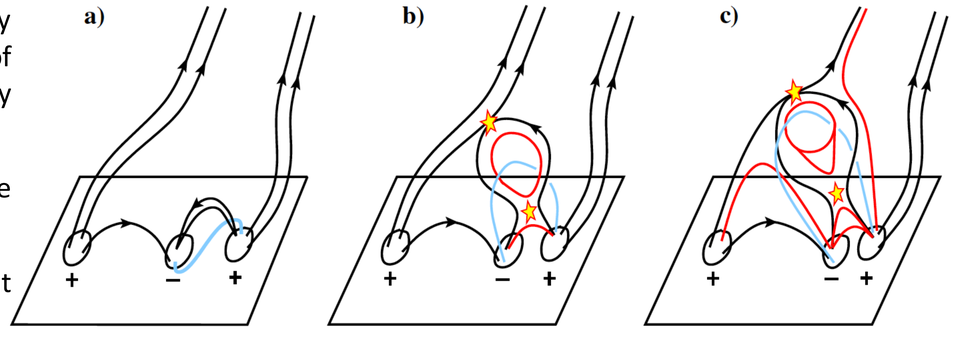

- We find in each of the ten jets that opposite polarity magnetic flux patches converge and cancel, with a flux reduction of 20-60 %.

Measured Parameters for the Observed Coronal Jets

Event No.	Date	Time[a] (UT)	Location[b] x,y (arcsec)	Jet Speed[c] (km s^{-1})	Jet Dur.[d] min.	Jet-base[e] Width (km)	Minifil. length[f] (±1700 km)	Φ values[g] 10^{19} Mx	% of Φ[h] reduction
J1	2012 Mar 22	04:46	-470,-100	100±30	15±5	10500±500	9800	1.6	52 ± 5.8
J2	2012 Jul 01	08:32	-44, 285	100±10	10±2	27000±500	25000	4.0	18 ± 6.8
J3	2012 Jul 07	21:31	-192,-180	120±15	14±3	16500±400	10500	–[i]	–
J4	2012 Aug 05[j]	02:20	-485, 190	140±35	10±3	22000±1000	31000	1.5	21 ± 6.0
J5	2012 Aug 10	23:03	-168,-443	125±15	15±2	16000±400	10000	0.9	57 ± 5.4
J6	2012 Sept 20	22:56	-158,-486	35±5	9±2	20000±500	36000	2.0	23 ± 4.6
J7	2012 Sept 21	03:33	-115, -485	135±30	12±1	17500±500	15000	1.0	36 ± 7.2
J8	2012 Sept 22	01:25	-338, 103	110±45	11±1	13000±600	5700	0.9	50 ± 5.1
J9	2012 Nov 13	04:21	-28,-307	55±5	9±3	18000±1000	25000	1.7	34 ± 3.2
J10	2012 Dec 13	10:36	26, 50	65±20	10±2	9500±500	12500	1.2	38 ± 5.0

References

- [1]Shibata, K., Ishido, Y., Acton, L. W., et al. 1992, PASJ, 44, L173
- [2]Raouafi, N. E, Patsourakos, S., Pariat, E., et al. 2016, SSRv, 201, 1
- [3]Sterling, A. C., Moore, R. L, Falconer, D. A., & Adams, M. 2015, Nature, 523, 437
- [4]Panesar, N. K., Sterling, A. C., Moore, R. L., & Chakrapani. P, 2016, ApJL, 832, L7

Acknowledgements: NKP is supported by an appointment to the NASA Postdoctoral Program at the NASA MSFC, administrated by USRA under contract with NASA. We also acknowledge the support from NASA HGI program, and use of SDO/AIA/HMI data.